

This is smaller than the out-of-plane γ_e values discussed in the following sections. Because this estimate is also small enough such that the corresponding $1.6/\gamma_{eL}$ is greater than 0.1, it is useful only for determining that either Section 4.6.2, Item 4b, should be satisfied, or a more rigorous estimate of γ_{eL} should be determined.

7.9 OUT-OF-PLANE ELASTIC CONSTRAINED-AXIS TORSIONAL AND LATERAL-TORSIONAL BUCKLING (CATB AND LTB) ANALYSIS CALCULATIONS

Figure 7-10 shows a model for calculation of the out-of-plane elastic buckling load ratio under axial compression, considering the doubly tapered roof girder design segment targeted in this example. It is expected that the out-of-plane buckling is governed by CATB about the outside (top) flange for this case. This is due to the intermediate out-of-plane lateral bracing of the top flange at the middle of the segment, whereas the bottom flange is laterally unsupported along the entire segment length. In addition to these CATB results, the results of a similar model employed to evaluate the elastic LTB load ratio for this design segment, γ_{eLTB} , are presented in the following.

For the model shown in Figure 7-10, flexural and warping continuity is released between this design segment and the adjacent unbraced lengths within the roof girder. The doubly tapered segment shown here is isolated from the overall frame and subjected to ideal torsionally and flexurally simply supported end conditions. The combination of the purlin bracing of the outside flange and the diagonal bracing to the inside flange, located at the ends of the segment, is assumed to prevent out-of-plane lateral displacement and twist. The end lateral displacement constraints as well as the torsional constraints are denoted by the black arrows with the slash through them. In addition, the roof girder is constrained (i.e., braced) out-of-plane at the intermediate purlin location on its top flange. This constraint is indicated by the black arrow with the slash through it shown at mid-length of the top flange. An axial load of 31.6 kips, equal to the largest value of the internal axial compression within the subject length, obtained from the load-deflection analysis results in Figure 7-5, is applied at the cross-section centroid at the righthand end of the segment. This load is indicated by a lighter-colored arrow without a slash at the righthand end. The forces and moments indicated by the other arrows are notional lateral loads and notional moments discussed in the following.

Given the geometry and support conditions illustrated in Figure 7-10, the out-of-plane elastic buckling capacity of the member is influenced significantly by major-axis bending induced by the axial loads. However, γ_{eCAT} pertains to the case of internal axial load with zero bending. Therefore, to obtain a rigorous solution for γ_{eCAT} using an elastic buckling analysis, notional lateral loads and notional moments must be applied at the locations of the pinch point and steps in the flange thicknesses in this problem. The notional lateral loads and the notional moments cancel the moments caused by the deviation of the member centroidal axis from a straight line (due to the steps in the cross section as well as the change in the web taper at the different locations along the member length).

As noted in Section 7.2, the bottom flange thickness steps from $\frac{1}{4}$ in. to $\frac{3}{8}$ in. at the pinch point, and the top flange thickness steps from $\frac{1}{2}$ in. to $\frac{1}{4}$ in. at 0.5 ft to the right of the pinch point. Figure 7-11(a) shows a free-body diagram of the subject length, subjected to concentrically applied axial forces at the design segment ends. Figure 7-11(b) shows the corresponding first-order internal moments employed in the elastic linear buckling analysis of this segment in the absence of notional lateral

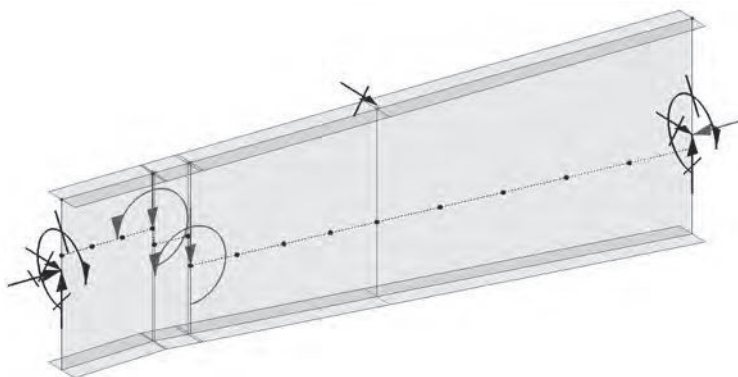
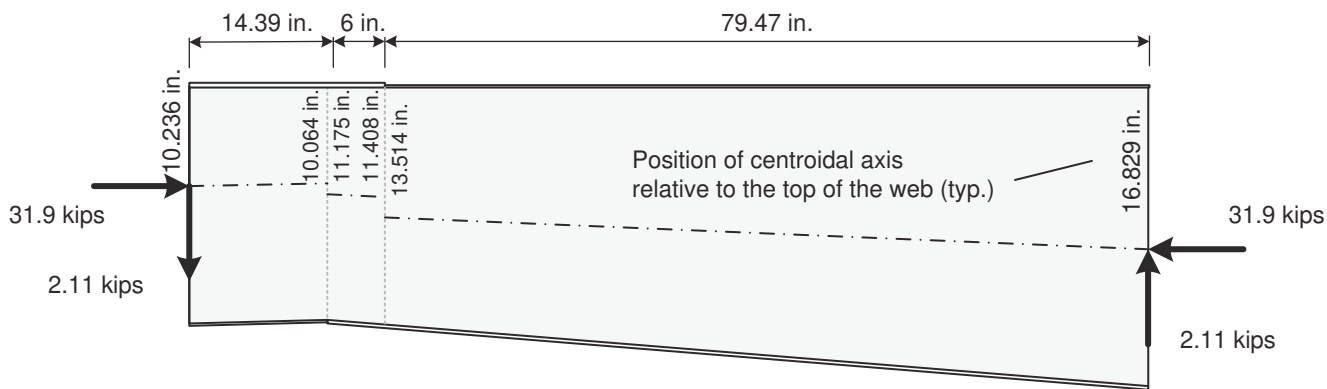
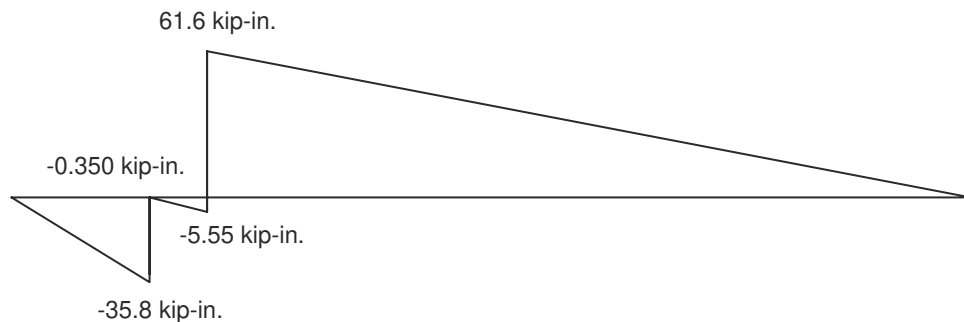


Fig. 7-10. γ_{eCAT} model for the subject doubly tapered roof girder design segment.

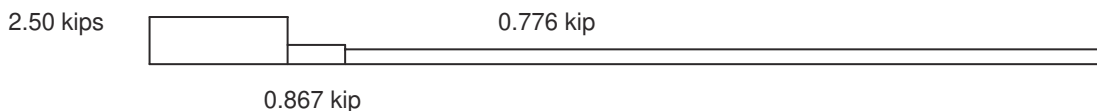
loads and moments. Figure 7-11(c) shows the notional shear forces necessary, along with concentrated notional moments at the two cross-section transition points, to generate the negative of the moment diagram shown in Figure 7-11(b). These shear forces are obtained by dividing the change in the moment along each of the partial member lengths by the corresponding length. Figure 7-11(d) shows the final notional lateral loads and notional moments required to cancel the internal bending moments due to the concentrically applied end axial loads, as well as the corresponding end reactions. The notional lateral loads are calculated as the difference in the internal notional shear forces at the cross-section transition points from Figure 7-11(c), and the notional moments are obtained as the difference in the internal moments at the transition points from Figure 7-11(b).



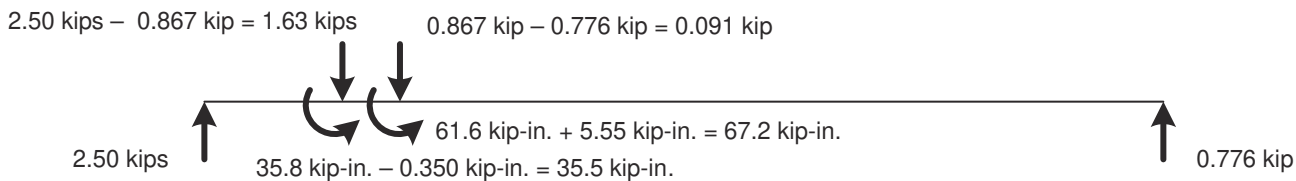
(a) Free-body diagram of subject length with centroidally applied end axial forces



(b) Internal moments produced by the concentrically applied end axial forces



(c) Notional internal shear forces corresponding to the negative of the internal moments in (b)



(d) Notional lateral loads and moments giving zero net internal moment, and corresponding end reactions

Fig. 7-11. Calculation of notional horizontal loads and notional moments required to cancel the bending effects due to concentrically applied end axial forces in the CATB analysis.

This is a preview. Click here to purchase the full publication.

The creation of a “pure axial load” condition for a member whose centroidal axis is not a straight line—such that (1) an out-of-plane buckling analysis for pure axial compression can be conducted, followed by (2) a separate out-of-plane LTB analysis of the member subjected to bending only, not considering any axial compression (as presented in the following discussions)—is a convoluted artifice of the ordinary member design approach of determining separate axial compressive and flexural strength ratios, then combining these ratios within a strength interaction equation. This separation of axial compression and flexure is sufficient, and lacks complications, for design of nominally straight members. The same cannot be said for the design of members that do not have a nominally straight centroidal axis. The inelastic buckling analysis solution shown subsequently in Section 7.15 avoids these complications by providing a direct assessment of the non-straight member subjected to the combined bending and axial compression.

Figure 7-12 shows the CATB mode for this problem. The buckling deflections are dominated by twisting about the top of the outside flanges (i.e., the location of the attachment of the purlins). The corresponding elastic buckling load ratio is $\gamma_{eCAT} = 10.5$. That is, this doubly tapered design segment theoretically bifurcates into the CATB mode at 10.5 times the internal axial forces associated with the required ASD load combination.

Figure 7-13(a) shows a free-body diagram of the subject roof girder design segment showing the applied loads employed to calculate the elastic LTB load ratio, γ_{eLTB} . The end moment values of 43.1 kip-ft and 118 kip-ft are the required ASD end moments obtained from Figure 7-4. The transverse load applied to the top flange is the component of the load transferred from the corresponding purlin perpendicular to the design axis. The other applied loads are the reverse of the notional loads calculated in Figure 7-11. These loads produce the effect of the estimated internal axial force of 31.6 kips acting through the changes in the orientation and offset of the member centroidal axis. The end shear forces in Figure 7-13(a) are determined from static equilibrium, given the previous applied loads. Figure 7-13(b) shows the internal moment diagram corresponding to these loads. This diagram is a close approximation of the moment diagram from Figure 7-4 for the subject length.

Figure 7-14 shows the LTB mode for the subject doubly tapered roof girder design segment. The displacement boundary conditions for this model are the same as those for the previous CATB model, and the shape of the buckling mode is very similar to that of Figure 7-12. However, in this case, the segment is subjected to applied loads producing the moment diagram from Figure 7-4 rather than loads producing pure axial compression equal to the values from Figure 7-5. (The reader might note that the notional loads from Figure 7-12 are applied in the opposite direction in this model, to generate the effect of the member axial force acting through the variations in the cross-section centroid along the length, and that the magnitude of these effects is relatively small compared to the other moments within the length of the design segment.) The subject roof girder design segment theoretically bifurcates elastically into the mode shown in Figure 7-14 at a load ratio of $\gamma_{eLTB} = 9.67$. That is, theoretical elastic LTB of this segment occurs at 9.67 times the required ASD internal moments. The corresponding solution using the moments determined using the ELM load-deflection analysis requirements is $\gamma_{eLTB} = 9.86$.

The reader might be interested in the sensitivity of γ_{eLTB} to the various details of the stepped and doubly tapered geometry of the subject design segment, because both steps in the cross section as well as the change in the taper angle occur within approximately 20% of the total segment length from its lefthand end. In addition, the reader might question whether the midlength lateral

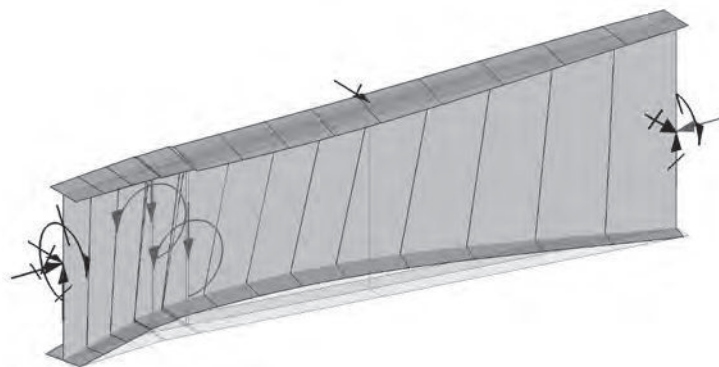
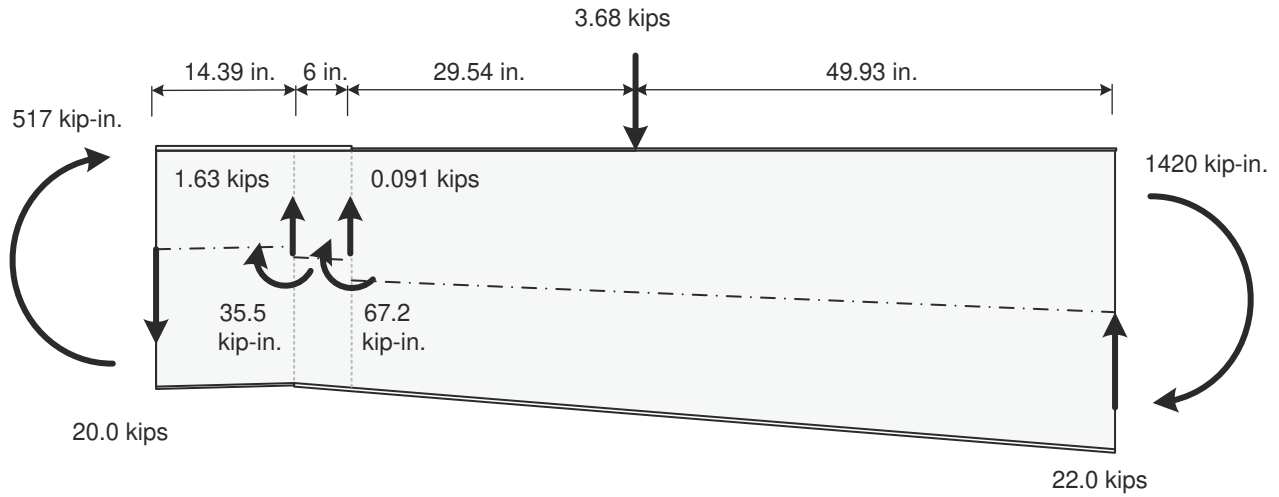
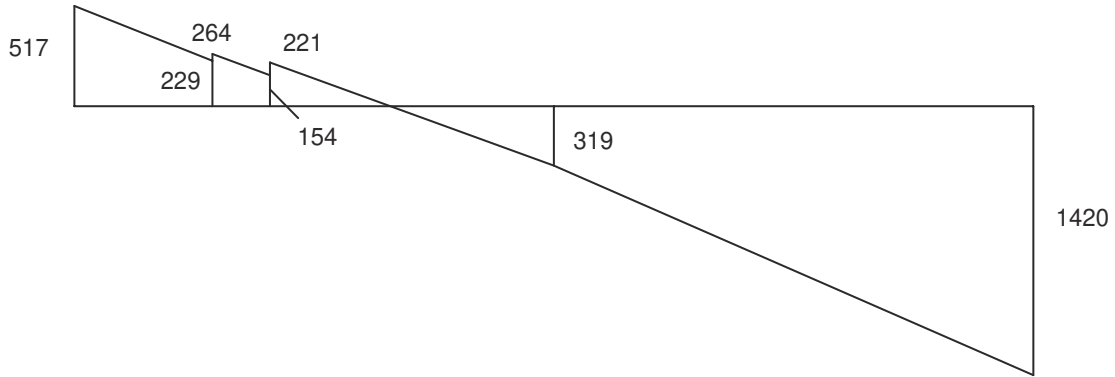


Fig. 7-12. CATB of the subject doubly tapered roof girder design segment at 10.5× the ASD required axial force.



(a) Free-body diagram of subject length showing forces applied to produce the required ASD internal moments



(b) Internal moment diagram (units: kip-in.) for subject unbraced length

Fig. 7-13. Free-body and moment diagrams for calculation of the elastic LTB load ratio, γ_{LTB} , for the subject doubly tapered roof girder design segment.

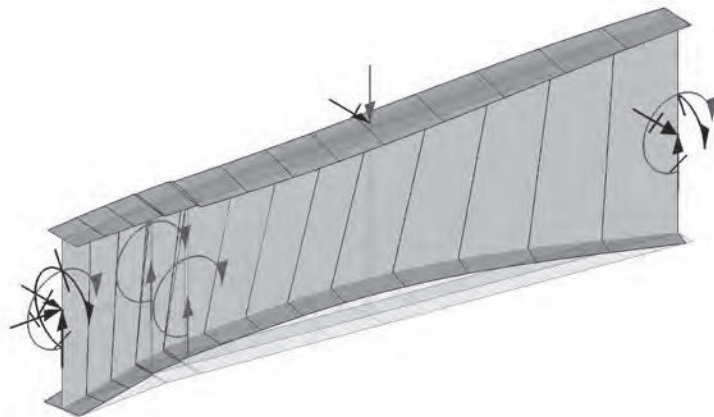


Fig. 7-14. Elastic LTB of the doubly tapered roof girder design segment at $9.67\times$ the ASD required internal moments.

brace at the top flange has any significant influence on the elastic LTB resistance for this problem. The following modified elastic buckling solutions are useful in addressing these questions:

- If the top flange brace is removed from the model with the DM loading, γ_{eLTB} is reduced to 9.48 (i.e., a reduction in capacity of only 2%).
- In addition, if the 6 in. \times $\frac{1}{4}$ in. top flange and the 6 in. \times $\frac{3}{8}$ in. bottom flange are extended over the full length of the design segment, eliminating the steps in the cross-section dimensions, γ_{eLTB} is reduced to 9.33, a total reduction of only 3.5%.
- Lastly, if the web taper is modified to a single linear taper from the maximum web depth of 31.2 in. at the righthand end to a minimum depth of 23.1 in. at the lefthand end (such that the geometry to the right of the pinch point is unchanged), γ_{eLTB} is reduced to only 9.24, a total reduction of only 4.4%.

7.10 MANUAL ESTIMATION OF γ_{eCAT} AND γ_{eLTB} FOR THE SELECTED DOUBLY TAPERED ROOF GIRDER DESIGN SEGMENT

The subject doubly tapered roof girder design segment has measurable steps in its top and bottom flange thickness in addition to its doubly tapered web geometry (Table 7-1). Therefore, this segment has substantial geometric complexity. A coarse estimate of the elastic buckling load ratio, γ_{eCAT} , of this segment can be obtained by applying Equation 5-10 with different cross sections along the segment length, taking P_{eCAT} as the smallest value from these calculations, then dividing P_{eCAT} by the largest value of the internal axial force along the segment length.

The cross section at the left end of the design segment gives the smallest value of P_{eCAT} . The corresponding calculations are as follows:

$$\begin{aligned} h_o &= h + t_{f1}/2 + t_{f2}/2 \\ &= 24.648 \text{ in.} + \frac{1}{2} \text{ in.}/2 + \frac{1}{4} \text{ in.}/2 \\ &= 25.0 \text{ in.} \end{aligned}$$

At the top flange:

$$\begin{aligned} I_{y1} &= \frac{t_{f1} b_{f1}^3}{12} \\ &= \frac{(\frac{1}{2} \text{ in.})(6 \text{ in.})^3}{12} \\ &= 9.00 \text{ in.}^4 \end{aligned} \tag{5-12}$$

At the bottom flange:

$$\begin{aligned} I_{y2} &= \frac{t_{f2} b_{f2}^3}{12} \\ &= \frac{(\frac{1}{4} \text{ in.})(6 \text{ in.})^3}{12} \\ &= 4.50 \text{ in.}^4 \end{aligned} \tag{5-13}$$

$$\begin{aligned} C_w &= \frac{h_o^2 I_{y1}}{\frac{I_{y1}}{I_{y2}} + 1} \\ &= \frac{(25.0 \text{ in.})^2 (9.00 \text{ in.}^4)}{\left(\frac{9.00 \text{ in.}^4}{4.50 \text{ in.}^4}\right) + 1} \\ &= 1,880 \text{ in.}^6 \end{aligned} \tag{5-11}$$

$$\begin{aligned}
 I_y &= I_{y1} + I_{y2} + \frac{ht_w^3}{12} \\
 &= 9.00 \text{ in.}^4 + 4.50 \text{ in.}^4 + \frac{(24.648 \text{ in.})(\frac{3}{16} \text{ in.})^3}{12} \\
 &= 13.5 \text{ in.}^4
 \end{aligned}$$

$$\begin{aligned}
 A &= (6 \text{ in.})(\frac{1}{2} \text{ in.}) + (24.648 \text{ in.})(\frac{3}{16} \text{ in.}) + (6 \text{ in.})(\frac{1}{4} \text{ in.}) \\
 &= 9.12 \text{ in.}^2
 \end{aligned}$$

$$\begin{aligned}
 a_c &= \bar{y} \\
 &= \frac{\frac{(6 \text{ in.})(\frac{1}{2} \text{ in.})^2}{2} + \frac{(\frac{3}{16} \text{ in.})(24.648 \text{ in.})^2}{2} + (6 \text{ in.})(\frac{1}{4} \text{ in.})\left(24.648 \text{ in.} + \frac{\frac{1}{4} \text{ in.}}{2}\right)}{9.12 \text{ in.}^2} + \frac{1}{2} \text{ in.} \\
 &= 10.7 \text{ in.}
 \end{aligned}$$

$$\begin{aligned}
 y_o &= \frac{t_f1}{2} + \frac{h_o I_{y2}}{I_y} - \bar{y} && (5-14) \\
 &= \frac{\frac{1}{2} \text{ in.}}{2} + \frac{(25.0 \text{ in.})(4.50 \text{ in.}^4)}{13.5 \text{ in.}^4} - 10.7 \text{ in.} \\
 &= -2.12 \text{ in.}
 \end{aligned}$$

$$\begin{aligned}
 a_s &= a_c + y_o \\
 &= 10.7 \text{ in.} - 2.12 \text{ in.} \\
 &= 8.58 \text{ in.}
 \end{aligned}$$

$$\begin{aligned}
 I_x &= \frac{(6 \text{ in.})(\frac{1}{2} \text{ in.})^3}{12} + (6 \text{ in.})(\frac{1}{2} \text{ in.})\left(10.7 \text{ in.} - \frac{\frac{1}{2} \text{ in.}}{2}\right)^2 \\
 &\quad + \frac{(\frac{3}{16} \text{ in.})(24.648 \text{ in.})^3}{12} + (\frac{3}{16} \text{ in.})(24.648 \text{ in.})\left(\frac{1}{2} \text{ in.} + \frac{24.648 \text{ in.}}{2} - 10.7 \text{ in.}\right)^2 \\
 &\quad + \frac{(6 \text{ in.})(\frac{1}{4} \text{ in.})^3}{12} + (6 \text{ in.})(\frac{1}{4} \text{ in.})\left(\frac{1}{2} \text{ in.} + 24.648 \text{ in.} + \frac{\frac{1}{4} \text{ in.}}{2} - 10.7 \text{ in.}\right)^2 \\
 &= 901 \text{ in.}^4
 \end{aligned}$$

$$\begin{aligned}
 r_x &= \sqrt{\frac{I_x}{A}} \\
 &= \sqrt{\frac{901 \text{ in.}^4}{9.12 \text{ in.}^2}} \\
 &= 9.94 \text{ in.}
 \end{aligned}$$

$$\begin{aligned}
 r_y &= \sqrt{\frac{I_y}{A}} \\
 &= \sqrt{\frac{13.5 \text{ in.}^4}{9.12 \text{ in.}^2}} \\
 &= 1.22 \text{ in.}
 \end{aligned}$$

$$\begin{aligned}
 J &= \frac{ht_w^3}{3} + \frac{b_{ft}t_{ft}^3}{3} \left(1 - 0.63 \frac{t_{ft}}{b_{ft}}\right) + \frac{b_{fc}t_{fc}^3}{3} \left(1 - 0.63 \frac{t_{fc}}{b_{fc}}\right) \\
 &= \frac{(24.648 \text{ in.})(\frac{3}{16} \text{ in.})^3}{3} + \frac{(6 \text{ in.})(\frac{1}{2} \text{ in.})^3}{3} \left[1 - 0.63 \left(\frac{\frac{1}{2} \text{ in.}}{6 \text{ in.}}\right)\right] + \frac{(6 \text{ in.})(\frac{1}{4} \text{ in.})^3}{3} \left[1 - 0.63 \left(\frac{\frac{1}{4} \text{ in.}}{6 \text{ in.}}\right)\right] \\
 &= 0.322 \text{ in.}^4
 \end{aligned} \tag{5-6}$$

$$\begin{aligned}
 P_{eCAT} &= \left[\frac{\pi^2 E (C_w + I_y a_s^2)}{L_{cz}^2} + GJ \right] \frac{1}{r_x^2 + r_y^2 + a_c^2} \\
 &= \left\{ \frac{\pi^2 (29,000 \text{ ksi}) [1,880 \text{ in.}^6 + (13.5 \text{ in.}^4)(8.58 \text{ in.})^2]}{(99.86 \text{ in.})^2} \right\} \left\{ \frac{1}{(9.94 \text{ in.})^2 + (1.22 \text{ in.})^2 + (10.7 \text{ in.})^2} \right\} \\
 &= 401 \text{ kips}
 \end{aligned} \tag{5-10}$$

The maximum required compressive strength toward the righthand end of the design segment is:

$$P_r = 31.9 \text{ kips}$$

$$\begin{aligned}
 \gamma_{eCAT} &= \frac{P_{eCAT}}{P_r} \\
 &= \frac{401 \text{ kips}}{31.9 \text{ kips}} \\
 &= 12.6
 \end{aligned}$$

This value is a reasonable rough estimate of the rigorous value of $\gamma_{eCAT} = 10.5$ determined from an elastic linear buckling analysis.

The elastic LTB load ratio for the subject doubly tapered roof girder design segment may be estimated using the procedure discussed in Appendix C.2. This procedure requires the calculation of the maximum ratio, f_r/F_{eLTB1} , as well as f_r/F_{eLTB1} at the quarter points and middle of the unbraced length under consideration. In this example, the unbraced length, L_b , should be taken as the overall length of the design segment = 99.86 in. (according to AISC *Specification* Appendix 6, Section 6.3.1) because the segment has a reversal in the sign of the bending moment and only the top flange is braced at the intermediate purlin bracing location. Upon calculating f_r/F_{eLTB1} at various points, one can determine that the maximum f_r/F_{eLTB1} occurs at the right end of the design segment in this problem. The elastic LTB stress of a prismatic unbraced length having the cross section at this location is determined as follows:

$$\begin{aligned}
 h_o &= h + t_{f1}/2 + t_{f2}/2 \\
 &= 31.173 \text{ in.} + \frac{1}{4} \text{ in.}/2 + \frac{3}{8} \text{ in.}/2 \\
 &= 31.5 \text{ in.}
 \end{aligned}$$

$$\begin{aligned}
 d &= h + t_{f1} + t_{f2} \\
 &= 31.173 \text{ in.} + \frac{1}{4} \text{ in.} + \frac{3}{8} \text{ in.} \\
 &= 31.8 \text{ in.}
 \end{aligned}$$

$$\begin{aligned}
 A &= (6 \text{ in.})(\frac{3}{8} \text{ in.}) + (31.173 \text{ in.})(\frac{3}{16} \text{ in.}) + (6 \text{ in.})(\frac{1}{4} \text{ in.}) \\
 &= 9.59 \text{ in.}^2
 \end{aligned}$$

$$\begin{aligned}
 h_c &= \frac{2 \left[\frac{(6 \text{ in.})(\frac{3}{8} \text{ in.})^2}{2} + \frac{(\frac{3}{16} \text{ in.})(31.173 \text{ in.})^2}{2} + (6 \text{ in.})(\frac{1}{4} \text{ in.}) \left(31.173 \text{ in.} + \frac{\frac{3}{8} \text{ in.}}{2} \right) \right]}{9.59 \text{ in.}^2} \\
 &= 28.7 \text{ in.}
 \end{aligned}$$

$$\begin{aligned}\frac{h_c}{t_w} &= \frac{28.7 \text{ in.}}{3/16 \text{ in.}} \\ &= 153\end{aligned}$$

The web at this cross section is slender. Therefore, the St. Venant torsional stiffness is neglected in the calculation of the elastic LTB stresses:

$$\begin{aligned}a_w &= \frac{h_c t_w}{b_{fc} t_{fc}} && (\text{Spec. Eq. F4-12}) \\ &= \frac{(28.7 \text{ in.})(3/16 \text{ in.})}{(6 \text{ in.})(3/8 \text{ in.})} \\ &= 2.39\end{aligned}$$

$$\begin{aligned}r_t &= \frac{b_{fc}}{\sqrt{12 \left(\frac{h_o}{d} + \frac{1}{6} \frac{a_w h^2}{h_o d} \right)}} && (5-31) \\ &= \frac{6 \text{ in.}}{\sqrt{12 \left[\frac{(31.5 \text{ in.})}{(31.8 \text{ in.})} + \frac{1}{6} \frac{(2.39)(31.173 \text{ in.})^2}{(31.5 \text{ in.})(31.8 \text{ in.})} \right]}} \\ &= 1.48\end{aligned}$$

$$\begin{aligned}I_x &= \frac{(6 \text{ in.})(1/4 \text{ in.})^3}{12} + (6 \text{ in.})(1/4 \text{ in.}) \left(31.173 \text{ in.} - \frac{28.7 \text{ in.}}{2} + \frac{1/4 \text{ in.}}{2} \right)^2 \\ &\quad + \frac{(3/16 \text{ in.})(31.173 \text{ in.})^3}{12} + (3/16 \text{ in.})(31.173 \text{ in.}) \left(\frac{31.173 \text{ in.}}{2} - \frac{28.7 \text{ in.}}{2} \right)^2 \\ &\quad + \frac{(6 \text{ in.})(3/8 \text{ in.})^3}{12} + (6 \text{ in.})(3/8 \text{ in.}) \left(\frac{28.7 \text{ in.}}{2} + \frac{3/8 \text{ in.}}{2} \right)^2 \\ &= 1,390 \text{ in.}^4\end{aligned}$$

$$\begin{aligned}S_{xc} &= \frac{I_x}{h_c/2 + t_{fc}} \\ &= \frac{1,390 \text{ in.}^4}{28.7 \text{ in.}/2 + 3/8 \text{ in.}} \\ &= 94.4 \text{ in.}^3\end{aligned}$$

From Figure 7-2, $L_b = 99.86 \text{ in.}$

$$\begin{aligned}F_{eLTB1} &= \frac{\pi^2 E}{\left(\frac{L_b}{r_t} \right)^2} && (5-30) \\ &= \frac{\pi^2 (29,000 \text{ ksi})}{\left(\frac{99.86 \text{ in.}}{1.48 \text{ in.}} \right)^2} \\ &= 62.9 \text{ ksi}\end{aligned}$$

From Figure 7-13(a), $M_r = 1,420$ kip-in.

$$\begin{aligned} f_r &= \frac{M_r}{S_{xc}} \\ &= \frac{1,420 \text{ kip-in.}}{94.4 \text{ in.}^3} \\ &= 15.0 \text{ ksi} \end{aligned}$$

For compression on the bottom flange:

$$\begin{aligned} \left(\frac{f_r}{F_{eLTB1}} \right)_{max} &= \frac{15.0 \text{ ksi}}{62.9 \text{ ksi}} \\ &= 0.238 \end{aligned}$$

Following the same calculation procedures, the corresponding ratios of the compression flange applied to elastic buckling stresses at the quarter points and mid-length locations A, B, and C are:

Compression on the top flange:

$$\begin{aligned} \left(\frac{f_r}{F_{eLTB1}} \right)_A &= \frac{3.41 \text{ ksi}}{56.3 \text{ ksi}} \\ &= 0.0606 \end{aligned}$$

Compression on the bottom flange:

$$\begin{aligned} \left(\frac{f_r}{F_{eLTB1}} \right)_B &= \frac{4.05 \text{ ksi}}{65.4 \text{ ksi}} \\ &= 0.0619 \end{aligned}$$

$$\begin{aligned} \left(\frac{f_r}{F_{eLTB1}} \right)_C &= \frac{10.0 \text{ ksi}}{63.7 \text{ ksi}} \\ &= 0.157 \end{aligned}$$

It should be noted that because the top flange is in compression at point A, F_{eLTB1} is based on the top flange $r_t = 1.40$ in. at that location. In addition, the reader should note that none of the flange areas or lateral bending moments of inertia change by more than a factor of 2.0 at the steps in the flange thickness (Table 7-1), and as discussed at the end of Section 7.9, the pinch point and the steps in the flange thickness occur approximately within 20% of the total segment length from its lefthand end.

Given the previous ratios, the LTB modification factor may be estimated as:

$$C_b = \frac{4 \left(\frac{f_r}{F_{eLTB1}} \right)_{max} \chi}{\sqrt{\left(\frac{f_r}{F_{eLTB1}} \right)_{max}^2 + 4 \left(\frac{f_r}{F_{eLTB1}} \right)_A^2 + 7 \left(\frac{f_r}{F_{eLTB1}} \right)_B^2 + 4 \left(\frac{f_r}{F_{eLTB1}} \right)_C^2}} \quad (5-29)$$

where the nonprismatic geometry factor, χ , is determined as follows, using the procedure discussed in Appendix C.2:

- The steps in the cross-section geometry all occur between the lefthand support and the lefthand quarter point of the unbraced length (point A). Therefore, from Appendix C.3, the smallest F_{eLTB1} from the cross sections between the lefthand end of the unbraced length and point B is employed for the F_{eLTB1} corresponding to point A. This value of F_{eLTB1} is already employed in the previous calculations.
- $\beta_1 = 1.50^\circ$ and $\beta_2 = 4.61^\circ$, based on the geometries detailed in Figure 7-2 and Table 7-1.
- $L_1 = 14.39$ in. and $L_b = 99.86$ in. (see Figures 7-2 and 7-13).
- $h_{min} = 24.275$ in. at the pinch point, and $h_{max} = 31.173$ in. at the righthand end of the unbraced length, based on the geometries detailed in Figure 7-2 and Table 7-1.

- $$I_{yT} = \frac{(\frac{3}{8} \text{ in.})(6 \text{ in.})^3}{12}$$

$$= 6.75 \text{ in.}^4$$

$$I_{yP} = \frac{(\frac{1}{4} \text{ in.})(6 \text{ in.})^3}{12}$$

$$= 4.50 \text{ in.}^4$$

$$\frac{I_{yT}}{I_{yP}} = \frac{6.75 \text{ in.}^4}{4.50 \text{ in.}^4}$$

$$= 1.50 > 1.0$$

And therefore:

$$r_l = -0.02|\beta_{max}| \left(1 - \frac{1}{I_{yT}/I_{yP}} \right) \tag{C-2b}$$

$$= -0.02(4.61^\circ) \left(1 - \frac{1}{1.50} \right)$$

$$= -0.0307$$

- Given these parameters:

$$r_{DT} = 0.02 \left(\frac{L_l}{L_b} \right) (\beta_1 + \beta_2) \left(1 - \frac{h_{min}}{h_{max}} \right)^2 \tag{C-3}$$

$$= 0.02 \left(\frac{14.39 \text{ in.}}{99.86 \text{ in.}} \right) (1.50^\circ + 4.61^\circ) \left(1 - \frac{24.275 \text{ in.}}{31.173 \text{ in.}} \right)^2$$

$$= .000863$$

- $\beta_1 + \beta_2$ is positive; therefore, $r_K = 0.0$. (C-4a)

- The unbraced length is subjected to reversed-curvature bending.

- From these parameters:

$$\chi = 1 + r_l + r_{DT} + r_K \leq 1.0 \tag{C-1b}$$

$$= 1 - 0.0307 + 0.000863 + 0.0$$

$$= 0.970 < 1.0$$

The subject unbraced length has steps in the cross-section dimensions in addition to the double taper of its web. Therefore, the χ value must be multiplied by the χ factor explained in Appendix C.3 to also account for the stepped geometry effects. The maximum shift in the shear center due to the steps in the cross-section geometry is (see Figure 7-2):

$$d_{Smax} = 10.549 \text{ in.} - 7.967 \text{ in.}$$

$$= 2.582 \text{ in.}$$

Therefore, the χ factor addressing the influence of the steps in the cross-section geometry is:

$$\chi = 1 - 9 \frac{d_{Smax}}{L_b} \tag{C-9}$$

$$= 1 - 9 \left(\frac{2.582 \text{ in.}}{99.86 \text{ in.}} \right)$$

$$= 0.767$$